# Diffusion of Ionic Fluorescent Probes atop Polyelectrolyte Brushes

Cunfu Zhang,[†,‡] Xiao Chu,[†,‡] Zhongli Zheng,[†,‡] Pengxiang Jia,[†,‡] and Jiang Zhao*[,†]

[†]Beijing Laboratory of Molecular Science, Institute of Chemistry, Chinese Academy of Sciences, Beijing 100190, China
[‡]Graduate School of the Chinese Academy of Sciences, Beijing 100049, China

S *Supporting Information*

ABSTRACT: The lateral diffusion of ionic fluorescent molecules atop polyelectrolyte brushes was adopted to probe the distribution of counterions of the polyelectrolyte brushes. With a combination of single molecule fluorescence techniques, fluorescence correlation spectroscopy and single molecule fluorescence imaging, the lateral diffusion of the ionic probes (sulforhodamine B, rhodamine 6G) at the top of the model polyelectrolyte brushes with the opposite charges, poly ([2-(methylacryloyloxyl)ethyl] trimethylammonium chloride) (PMETAC) and polystyrene sulfonate (PSS), was studied with different external salt concentrations. A huge decrease of the diffusion rate of the probes was observed at salt concentrations 2−3 orders of magnitude lower than that for any detectable change of brushes thickness could be observed. The results reflect the early collapse of the top portion of the polyelectrolyte brushes and also the penetration of the probes into the brushes due to the increase of osmotic pressure by the salt level in the solution. The diffusion of the fluorescent counterion can serve as a very sensitive probe of the structure atop the polyelectrolyte brushes.
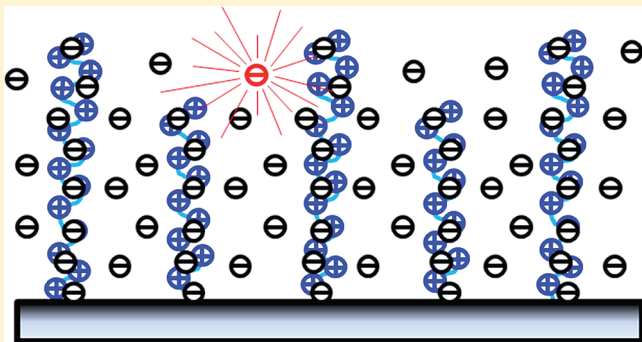
INTRODUCTION

Polyelectrolyte brushes are charged polymer chains end-grafted to solid surfaces with a high enough grafting density. They are emerging new approaches of surface modification with potential applications in colloidal stabilization, biological lubrication, biosensors, fluid controls in micro- and nanofluidic devices, and advanced drug delivery, and so forth.[1−3] Polyelectrolyte brushes have also been proven to be capable to immobilize proteins with their native structures and functions well-preserved and therefore are believed to serve as substrates for biological processes and reactions.[4−6] Polyelectrolyte brushes have been attracting intensive attention for decades, and there have been increasing efforts to fabricate brushes with new functionalities and also to investigate their physical properties and structures.

Studies have shown that counterions are playing a very important role in determining the structure of polyelectrolyte brushes. Different from neutral polymer brushes, in which the stretching of the polymer chains is due to the osmotic pressure generated by the dense chain segments, the driving force for the charged polymer chain to stretch in polyelectrolyte brushes is the osmotic pressure from the counterions, when the grafting density and charge density is high enough (modeled as osmotic brushes).[7,8] The swelling of polyelectrolyte brushes is affected by the presence of external salts—when the salt concentration outside the brushes is higher than the concentration of counterions inside the brushes, the transition from the osmotic brushes to the salted brushes takes place.[7−9]

The properties of counterions inside polyelectrolyte brushes have been attracting research attention. Theories, simulations, and experiments have shown that the distribution of counterions in polyelectrolyte brushes is nonuniform, depending on the location in the direction normal to the surface.[10−12] The dynamics of the counterions is another essential aspect because it should rely pretty much on the structure of the brushes and can serve as a sensitive probe for the structure, for example, the electric potential profile distribution, the density of chain segments, and so forth. Therefore, it should be helpful if any experimental method can be applied to study this question. By using charged fluorescent molecule as probes for counterions and adopting single molecule fluorescence techniques as the sensitive methods, the diffusive motion of single anionic fluorophores has been studied.[13] In the current study, we adopted the idea of using ionic fluorophores as probes for counterions of the charged brushes and studied the diffusion of the probes with the brushes under different salt concentrations in the solution. The results show that the diffusion rate of the counterion probes changes at salt concentrations 3 orders of magnitude lower than that of noticeable change of the brush thickness is detected by macroscopic methods. The results impose new information on the counterion distribution of polyelectrolyte brushes.
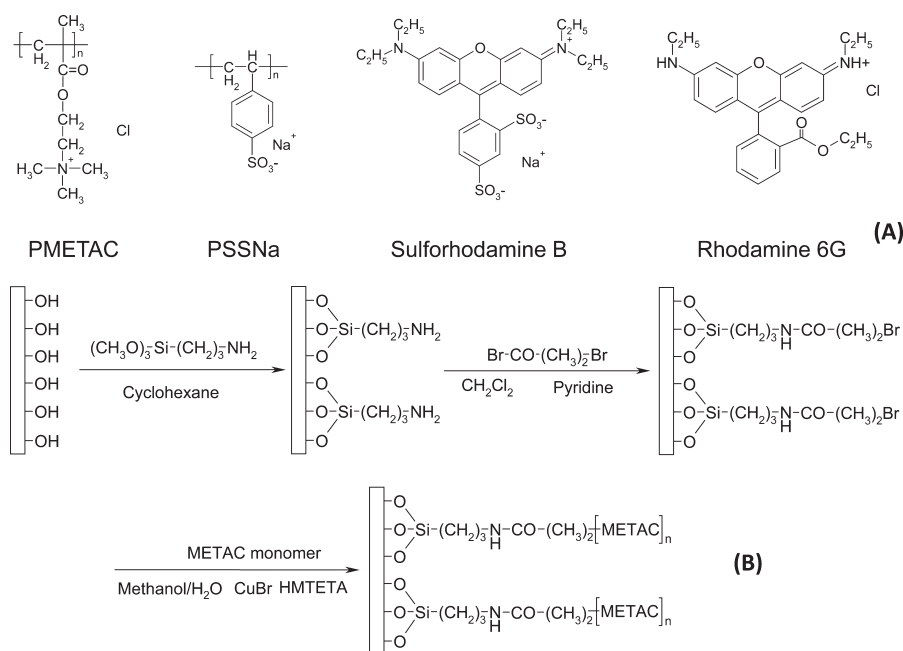
Figure 1. Panel A: The chemical structures of poly([2-(methylacryloyloxyl)ethyl] trimethylammonium chloride) (PMETAC), sodium polystyrene sulfonate (PSSNa), sulforhodamine B, and rhodmine 6G. Panel B: Schematic illustration of the fabrication of the PMETC brushes on silica surfaces.

■ EXPERIMENTAL SECTION

The experimental investigations were conducted in the following way. PMETAC brushes, poly([2-(methylacryloyloxyl)ethyl] trimethylammonium chloride), and sodium polystyrene sulfonate (PSSNa) brushes were adopted as the model systems. The chemical structures of these two polymers are illustrated in Figure 1A. Charged fluorescent molecules, sulforhodamine B and rhodamine 6G, were used as probes for counterions (Figure 1A). To observe and measure the diffusion rate of tracer counterion probes at the brushes, total internal reflection fluorescence microscopy (TIRFM) and fluorescence correlation spectroscopy (FCS) with single molecule sensitivity were employed.

Materials. Surface-initiated atom transfer radical polymerization (ATRP) was used to fabricate PMETAC brushes on solid substrates (silicon wafers and fused silica slips). Figure 1B is the illustration of the reaction scheme. Before fabrication, the substrates were carefully cleaned by multiple steps, such as ultrasonication in organic solvents and oxygen plasma treatment to remove adsorbed organic substances. The substrates were further treated in piranha solution (H_2O_2/H_2SO_4 = 3:1) at 110 °C for 30 min to create hydroxyl group-rich surfaces. *Caution: Piranha solution is extremely corrosive, and special care should be taken while handling it.* To anchor initiators to the surface, self-assembled monolayers of 3-aminopropyl trimethoxysilane (APTMS) were first fabricated in its cyclohexane solution. The initiator was then tagged onto this monolayer by reaction of this precoated surface with 2-bromoisobutyl bromide (2-BiB). After the initiator monolayers were prepared, a surface-initiated ATRP reaction was conducted in methanol solution of METAC monomer inside sealed chambers copiously prepurged with nitrogen of high purity.

PMETAC brushes were prepared by surface-initiated ATRP. METAC monomer (1.54 mL, 6.4 mmol) and 1,1,4,7,10,10-hexamethyltriethylene tetramine (HMTETA, 22 μL, 0.08 mmol) were dissolved in a 12 mL mixture of methanol and deionized water (3:1 v/v). The solution was degassed by three freeze−pump−thaw

cycles. Then, CuBr (11.44 mg, 0.08 mmol) was added, and the mixture was degassed by another three freeze−pump−thaw cycles. After ultrasonication for 2 min, this mixture turned into a homogeneous solution with light blue color. This solution was then transferred into a reaction chamber containing the target substrates precoated with initiator monolayers. Polymerization was conducted at room temperature under a nitrogen environment. After a desired amount of reaction time, substrates were removed from the solution and rinsed with the mixture of water/methanol (15:85 v/v) for 12 h in a Soxhlet extractor to remove any possible free unanchored polymers.

PSSNa brushes were prepared by the sulfonation of polystyrene (PS) brushes prepared by the grafting-to method. To prepare PS brushes, a self-assembled monolayer of expoxyl group terminated silane was first prepared on silica substrates, by immersing the substrates in 1% cyclohexane solution of 5,6-epoxyhexyl triethoxysilane (Gelest). Afterward, a thin film of amino-terminated polystyrene (PS, M_w = 120 × 10^3 g·mol^{-1}, M_w/M_n = 1.04, purchased from Polymer Source) was deposited on this precoated substrates using the PS toluene solution with a concentration of 1%. This sample was incubated at 160 °C under vacuum for 24 h. Later, the sample was vigorously rinsed with toluene by Soxhlet extraction for 5 h to remove physically adsorbed PS.

The PS brushes were sulfonated by a published protocol,[14] as briefly described below. First, acetyl sulfate was prepared by adding concentrated sulfuric acid (3.6 mL, 0.064 mol, 95%) to a mixture of acetic anhydride (10.2 mL, 0.108 mol) and 1,2-dichloroethane (49.8 mL) in an ice bath. Second, this mixture was added slowly into a reactor containing PS coated substrates. The reactor was heated to 60 °C for 5 h; the reaction was terminated, and the sample was rinsed with ethanol. By this process, the PS brushes were turned into polystyrene sulfonic acid brushes, which was later neutralized into polystyrene sulfonate sodium in NaHCO₃ (0.5 M) solution. At the final stage, the PSSNa brushes were rinsed in a Soxhlet extractor in deionized

15168

dx.doi.org/10.1021/jp204612u |*J. Phys. Chem. B* 2011, 115, 15167–15173

water for 4 h to remove the residual salts. The degree of sulfonation was estimated to be ∼60% by referring to the published data.[14] The thickness characterization of PSSNa brushes was conducted using an ellipsometer (M-2000V, J. A. Woollam), equipped with a liquid sample cell.

Thickness and Morphology Characterization of PMETAC Brushes. An atomic force microscope (AFM) with an aqueous environment was adopted for brush layer characterization. The AFM (Digital Instruments Nanoscope IIIA) was equipped with a liquid sample cell under the tapping mode using either silicon tips (spring constant = 27.3−52.7 N/m) or silicon nitride tips (spring constant = 1.45−1.51 × 10^{−3} N/m). The swelling process of the PMETAC brushes was characterized in situ by conducting observations at one exact location on the sample's surface, for both the "dry" and "wet" brushes. The brush thickness was determined by measuring the step height of a scratch in the brush layer created by a blade. Prior to each measurement, the sample was incubated in NaCl solution of a specified concentration for 40 min to reach its equilibrated state. Measurements were conducted carefully to prevent artifacts: (1) The measurements were performed at low salt concentrations first, and the salt concentration was tuned gradually to a higher level. (2) The salt solutions were prepared and stored in glassware made of silica so that the dissolution of ions from glassware is prevented. (3) For all experiments, the amplitude of "set-point" values of AFM for imaging, which effectively determined the force exerted to the brushes by the tips, was identically low so that ambiguities in thickness determination can be diminished.[15]

Fluorescence Correlation Spectroscopy (FCS) and Total Internal Reflection Fluorescence Microscopy (TIRFM). For the measurements of diffusion rate of fluorescent ionic probes, liquid sample cells were constructed, as illustrated by Figure 2. The cell was composed of a silica slide of 1.0 mm thickness grafted with polyelectrolyte brushes, a thin microscope cover slide, and spacers. Two tiny openings were drilled for the introduction and drainage of the salt solution. The sample cell was first filled with deionized water so that the brushes were swelled and equilibrated. Afterward, a very dilute solution (∼10^{−14} M) of fluorescent probes was injected, and sufficient incubation time was allowed for the thorough adsorption of the fluorescent probes. At the final stage, a copious amount of deionized water was rinsed through the sample cell to remove any residual unadsorbed fluorescent probes in the solution. After the measurement at salt-free conditions was finished, the salt level in the solution was raised by rinsing the sample cell with sufficient amounts of NaCl solution at a specific concentration. The salt concentration was gradually increased by rinsing the cell with NaCl solution of higher concentrations.

FCS measurements were conducted with a home-built system. The setup was constructed on an inverted microscope (Olympus IX-71) equipped with a water-immersion objective lens (Plan Apochromat 60×, numerical aperture = 1.2). The excitation light source is the 532 nm output of a solid-state laser, and the fluorescence excitation and collection were conducted at the confocal geometry. The background noise was greatly suppressed by a combination of a dichroic mirror and optical filters (Chroma Tech). The fluorescence was split into two parts of identical intensity, which were detected separately by two single photon counting modules (Hamamatsu, Japan). The fluorescence photon count signal was coupled into a multichannel FCS data acquisition board, and the data analysis was conducted by its software (ISS, USA).[16]
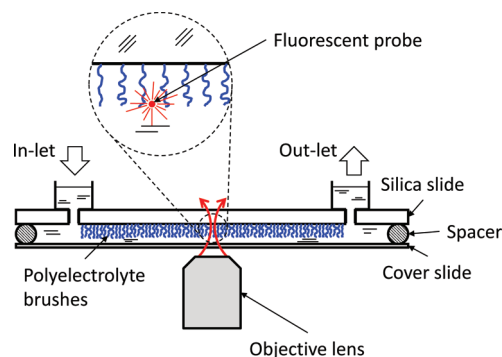
Figure 2. Schematic illustration of the sample cell for FCS measurements. The thickness of the spacer is about 100 μm.

The FCS technique measures the diffusion of fluorescent molecules by monitoring fluorescence fluctuation within the excitation-detection volume and by the analysis of the autocorrelation function of the fluctuation: $G(\tau) = (\langle F(t) \cdot F(t + \tau) \rangle)/(\langle F(t)^2 \rangle)$, where $F(t)$ denotes the fluorescence intensity at a certain time of t.[17−20] Numerical fitting of the autocorrelation function using appropriate models can give correct values of the diffusion coefficient and average concentration. For the case of in-plane diffusion, a two-dimensional Gaussian model is applied: $G(\tau) = 1/(\pi w_0 \langle \rho \rangle)((1 + 4D\tau)/(w_0^2))^{-1}$, where $\langle \rho \rangle$ is the average surface concentration of the fluorescent objects and D is the diffusion coefficient. w_0 is the lateral radius of the excitation and detection spot, and its value was approximately 220 nm at 20 °C, as calibrated by measuring standard substance with a known diffusion coefficient, such as rhodamine 6G and fluorescein. The FCS method has been proved to be very powerful in measuring the diffusion of fluorescent tracers at concentrations down to $10^{−9} − 10^{−12}$ M, in bulk solution as well as at interfaces. Although there is a concern about the possibility of the distortion of the excitation-detection volume (the point spread function) from the assumed Gaussian profile, it is less possible because the laser beam was illuminated from the solution side and the measurement on the brushes surface should not suffer from the possible distortion.

TIRFM observation was conducted on another setup. The excitation laser beam (532 nm) was introduced to the sample surface from the back of the substrates by an oil-immersion objective lens (Plan Apo, 100×, numerical aperture = 1.45).[21] By optimizing the incident angle, the laser beam was totally reflected at the surface coated with PMETAC brushes, and fluorescence was excited by the evanescent wave at the surface. After the background radiation was filtered by an optimized optical filter set, the fluorescence images were recorded by an electron multiplying charge-coupled device camera (Andor DV887) with the exposure time of 200 ms.

■ RESULTS AND DISCUSSION

Swelling and Collapse of the Polyelectrolyte Brushes in Aqueous Solutions. The characterization of thickness by AFM was conducted in situ at an exact same location at the edge of a scratch created by a blade. The section profile is shown in Figure 3. The original thickness of the brush without solution, the "dry" brush, was 19.0 nm.

The thickness of the swelled brushes (i.e., the "wet" brushes) was about 202.2 nm, showing a vast swelling of the PMETAC

brushes—a ratio of ∼10.6. This ratio is quite large, indicating the high extent of stretching of the PMETAC chains. This can help us to estimate the grafting density of the brushes. (Normally, the grafting density characterization is conducted using the method of sacrificial initiator.[22] However, because the determination of molecular weight of permanently charged polyelectrolytes is not as accurate as neutral polymers by ordinary methods as chromatography, the determination of the grafting density of polyelectrolyte brushes prepared by the grafting-from method has been rather difficult.) In the current case, because the swelling ratio is very high, a rough estimate of the grating density can be performed, by considering a fully stretched conformation of the chains. For a polyelectrolyte brush system with the grafting density of σ and a degree of polymerization of N, the total mass within a unit area is written as $(\sigma \cdot N \cdot m)/(N_A)$, where N_A is the Avogadro constant and m is the molecular weight of the repeating unit (the monomer). The thickness of the same system after solvent is removed (the "dry" brushes) is $(\sigma \cdot N \cdot m)/(N_A \cdot \rho)$, where ρ is the density of the solid polymer (∼1.32 g·cm^{-3}). The swelling ratio ($\gamma = 10$) is then expressed as $\gamma = (N \cdot b)/((\sigma \cdot N \cdot m)/(N_A \cdot \rho)) = (b \cdot N_A \cdot \rho)/(\sigma \cdot m)$, with b being the length of the monomer (0.25 nm). The estimation gives the value of the grafting density of 0.1 chain·nm^{-2}. This is a reasonable value compared with most polymer brushes prepared by the "grafting from" method. This value also agrees with the results of experiments using the sacrificial initiators (please refer to Supporting Information).

When NaCl solution was introduced, the thickness of the "wet" brushes decreased with the increase of salt concentrations. Figure 4A shows the data of the thickness (d) for PMETAC brushes as a function of the NaCl concentration (c_s). The thickness of swelled brushes is constant (∼200.0 nm) below the salt concentration of 2.5×10^{-4} M. There is a moderate change to 185.0 nm for salt levels lower than 2.5×10^{-3} M. Upon a further increase of NaCl concentration, the thickness starts to decrease considerably and reaches the value of 69.2 nm at the salt concentration of 1.0 M. The decrease of the thickness with the increase of salt concentration can be fitted pretty well with a power law of -0.14, as denoted by the blue line in Figure 4A ($d \propto c_s{}^{\nu}$). This dependence is much smaller than the $-1/3$ power law, as previously predicted by mean field theory[7,8] and observed by experiments with surface force apparatus[9] and neutron reflectivity.[23] We attribute this to the difference of the thickness characterization methods. Compared with other measurements, for example, the surface force apparatus, the thickness measurements by AFM are more affected by the forces exerted to the brushes by the AFM tips—the small radius of curvature of the AFM tips brings about a larger pressure to the brushes.[24,25] Therefore, the brushes are more compressed at low salt concentrations (when the chains are more expanded) than that at high salt concentrations (when the chains are contracted). Another possibility is the effect of excluded volume due to the big side groups of PMETAC chains, compared with other systems as PSS.[9,23] The polydispersity of the PMETAC system is an important factor, as discussed below.

The grafting density of PSS brushes was determined to be 0.08 nm^{-2}, with the parameters of the PSSNa known, such as the molecular weight, the density, and the dry brushes thickness. Figure 4B displays the data of thickness for the swelled PSS brushes, as measured by ellipsometry. The thickness starts to decrease at an NaCl concentration of 0.1 M, and the decrease of thickness changes upon the increase of salt concentration with a
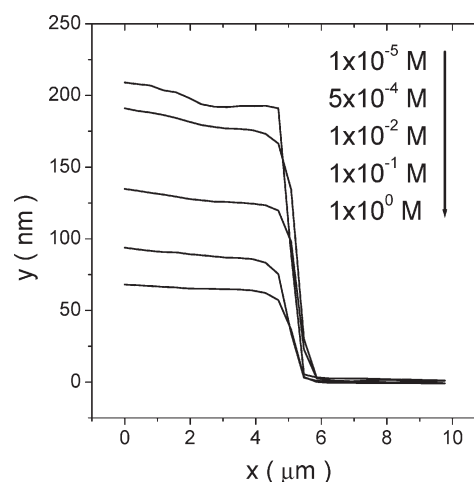
Figure 3. Results of a section analysis on a scratch created on the PMETAC brushes layer under different concentrations of NaCl in the solution. The thickness of the original "dry" brushes (without aqueous solvent applied) was 19.0 nm.
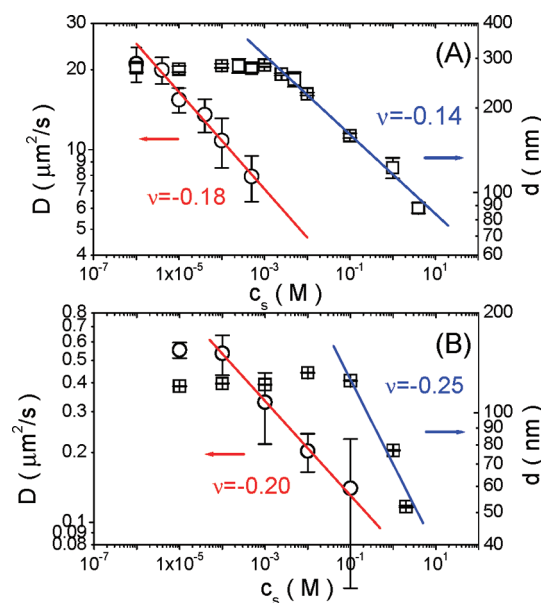
Figure 4. Thickness (d) of the "wet" polyelectrolyte brushes and diffusion coefficient (D) of fluorescent ionic probes as a function of NaCl concentration (c_s). Panel A: PMETAC brushes; Panel B: PSS brushes. The thickness of the "dry" PMETAC and PSS brushes is 26.0 nm and 20.0 nm, respectively.

power index of -0.25 (denoted by the blue line in Figure 4B). This value is close to $-1/3$, different to that of PMETAC brushes. This demonstrates the advantage of the intact manner of the ellipsometry measurements. Another factor considered for the difference between the data of PMETAC and PSSNa brushes is the uniformity of the chain length—PMETAC is polydispersed, while PSS is monodispersed. The polydispersity of PMETAC system brings about a much lower density at the outer rim of the brushes, which experiences a change of thickness at a much lower salt concentration, compared with the monodispersed PSS system.

Diffusion of Fluorescent Ionic Probes at the Polyelectrolyte Brushes. The diffusion of sulforhodamine B with the PMETAC

brushes was clearly observed by both TIRFM and FCS. The fluorescence images and videos show that a large amount of fluorescent probes was immobilized at the surfaces. These fixed probes were quickly photobleached by the laser radiation, as observed by a sharp decrease of the fluorescence intensity with prolonged laser illumination. After most of the immobilized fluorophores were photobleached, the optimum image contrast was reached, and the diffusive motion of individual fluorescent probes was clearly visualized. The video showing the diffusion of sulforhodamine B in PMETAC brushes is provided in the Supporting Information.

The trajectories of the moving fluorescent probes are rather difficult to determine because the single-to-noise ratio is not high enough to track these fast diffusing molecules. Therefore, the determination of diffusion coefficient was done through FCS measurements. Similar to TIRFM observations, a very high fluorescence intensity was detected when the laser spot of the FCS setup was initially adjusted onto the brushes, and this fluorescence intensity decreased to ∼1/5 of its original value within a few seconds. When the fluorescence intensity stabilized, the lateral diffusion of the probes was clearly measured (data shown in Figure 5). Control experiments were conducted to ensure that the measured diffusion was exclusively from the brush layer and not from the solution because no fluorescence signal and correlation data were detected when the focus was adjusted into the solution. Special steps were taken to guarantee the absence of residual fluorescent probes in the solution by rinsing the sample cell with NaCl solution at specific concentrations. When detachment of the probes were caused by the rinsing, the reload of the probes was performed by inject probe's NaCl solution of the same concentration. Although the control experiments can discriminate between measurements in solution and at interfaces, it does not guarantee a spatial resolution within the brushes because the resolution in the direction of the surface normal (along the optical axis of the objective lens) is $1-2 \mu m$, much larger than the brush thickness. Meanwhile, because of this fact, the possible contribution of the diffusion across the direction normal to the layer surface is excluded. Careful measurements were conducted by using the very low excitation intensity to prevent artifacts and errors brought by the photobleaching process. Measurements of dependence of the diffusion coefficient on the excitation intensity were conducted (data shown in the Supporting Information), and the value of diffusion coefficient was found to be almost constant at the laser intensity at the sample lower than $10 \mu W$, corresponding to a power intensity of $0.31 \times 10^8 W \cdot m^{-2}$. The measurements were performed mostly at the intensity of $5 \mu W$ ($0.15 \times 10^8 W \cdot m^{-2}$). The FCS curves deviate slightly from the single component fitting and therefore exhibit multiple modes (Figure 5), and this is attributed to the nonuniformity of the brushes—the difference between the inner and outer part of the brushes, which has been reported by previous studies.[13]

The dependence of the lateral diffusion coefficient (D) of the anionic fluorophores on PMETAC brushes as a function of salt concentration is shown in Figure 4A. The value of D is ∼22.0 $\mu m^2/s$ at a salt concentration of 1×10^{-6} M, and it starts to decrease with the increase of the salt concentration—the D value reaches ∼8.0 $\mu m^2/s$ at the salt concentration of 5×10^{-4} M. Accompanying the decrease of diffusion rate is a reduction of the number of the diffusive probes in the samples, as exhibited by the decrease of the overall fluorescence intensity and the increase in fluctuation amplitude. At salt concentrations higher than 5×10^{-4} M, the fluorescence signal from the sample was too weak to
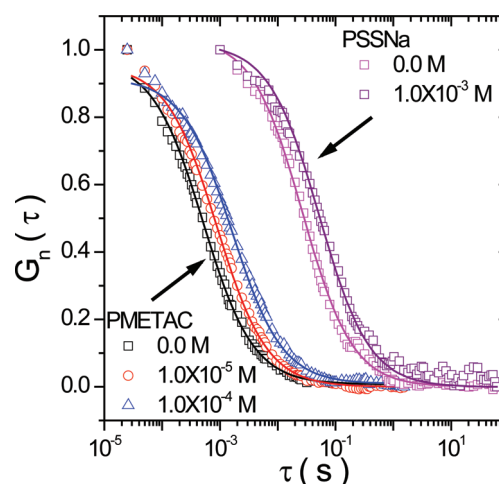
Figure 5. Normalized autocorrelation function of sulforhodamine B diffusing atop the PMETAC brushes, rhodamine 6G diffusing atop the PSS brushes under different salt concentrations. The values of the salt concentration are displayed by the data.

allow feasible FCS measurement. The decrease of the signal is due to the detachment of the probes from the brushes by the elevated salt level, similar to the release of protein by salt level.[4−6] A control experiment of measuring the diffusion of the probes in concentrated NaCl solution shows no change of the fluorescence intensity, which helps to exclude the possible effect of the interaction of the probes and the ions. Experiments with another anionic fluorescent molecule, sulforhodamine G, show similar behavior (details provided in the Supporting Information).

The diffusion rate of the cationic rhodamine 6G at anionic PSS brushes was also found to decrease with the elevation of salt concentration but with different features (data provided in Figure 4B). First, the D value of the probe is 0.55 $\mu m^2/s$, much lower than the case of PMETAC brushes. Second, the D value starts to decrease monotonously at a salt concentration of 1×10^{-4} M and reaches the value of 0.15 $\mu m^2/s$ at salt concentration of 0.1 M. This range for the change of D value is more than 2 orders of magnitude higher than the case of the PMETAC brushes. The change of D value with salt concentration follows a power index of -0.20 (denoted by the red line in Figure 4B), which is very close to that observed in the PMETAC system. In both systems, the most interesting feature is the vast decrease of the diffusion coefficient of the ionic probes, while the thickness of the brushes does not change very much: for the PMETAC system, the concentration range is 1×10^{-6} M $< c_s < 1 \times 10^{-3}$ M (Figure 4A), and for the PSS system, it is 1×10^{-4} M $< c_s < 1 \times 10^{-1}$ M (Figure 4B). Compared with the salt concentration at which the thickness starts to change, they are 3 orders of magnitude lower for both systems.

Where are the probes located with respect to the brush layer, inside or on the top of the brushes? It is difficult to determine the location of the probes by optical measurements because the spatial resolution of the microscope in the direction normal to the brush layer is around $1-2 \mu m$, much larger than the thickness of the brushes. However, the diffusing probes are considered to be located at the top of the brushes because the inner part of the brushes is too dense to allow fast diffusion. By the value of the grafting density (∼0.1 nm^{-2}), the polymer concentration inside the brushes is ∼10^2 mg/mL. The probes within such a dense

15171

dx.doi.org/10.1021/jp204612u |*J. Phys. Chem. B* 2011, 115, 15167–15173

environment should either be immobilized or diffusing very slowly, and it is beyond the lowest limit of the FCS measurement ($\sim 10^{-2}$ $\mu m^2/s$). The immobilized probes are clearly visualized in the single molecule imaging. Also, the large extent of photobleaching when the laser was initially focused onto the sample indicates the existence of immobilized or slowly moving fluorescent probes. The fast diffusing probes are located atop the polydispersed PMETAC brushes, and this is in agreement with previous studies showing that, for a polydispersed system, the distribution of the counterions can extend away from the brushes into the solution. Even for monodispersed brushes whose counterions are confined inside, as demonstrated by both mean field theory and experiments, the top portion can have a lower chain density compared with the inner part due to the thermo-motion of the chain end, allowing the existence of a small portion of counterions at the top. The difference in the absolute values of diffusion coefficient of the probes on these two systems also supports this picture. The counterions of the polydispersed PMETAC brushes extend into the solution and experience a less dense environment. For the monodispersed PSS brushes, the distribution of the counterions is much more restricted, and the surrounding of the counterions at the top portion of the brushes is denser. This brings about the big difference in the absolute values of the diffusivity.

It is excluded that the retardation of the probes' diffusion by salt addition originates from a strengthening of the interaction between the probe and the brushes. (1) The electrostatic interaction is weakened by the increase of salt concentration. (2) The hydrophobic interaction can be enhanced by addition of Hofmeister ions in the aqueous solution.[26−29] Provided that this is the origin, the retardation of the probes' diffusion should occur in similar ranges of salt concentration. This differs from the experimental observation, which shows that the salt concentration for the change of diffusion rate for the PMETAC and PSS systems differs by 2 orders of magnitude, excluding this possibility. (3) The similar behavior of the change of the probes' diffusivity with these two different systems helps to exclude the effect of specific binding of the probe with the brushes.

The slowing down of the probes' diffusion indicates an increase of segmental density of the polymer chains surrounding the probes. This can be either that the chain segments around the probes become denser or that the probes enter the inner part of the brushes with a higher density of chain segments. The former indicates a nonuniform collapse of the brushes, and the latter indicates that the counterions are driven into the brush layer by the elevated osmotic pressure by the external salt. Previous studies have shown that the outer part of the polyelectrolyte brush layer is more sensitive to the change of the salt level and pH value for the swelling and collapse—the outer portion of the brushes collapses at lower salt concentration than the inner portion does.[30,31] When this nonuniform collapse occurs, the density of the chain segments becomes higher while the inner part is not affected, and this denser environment makes the diffusion of the probes slowed down. The increase of the salt concentration in the solution imposes a higher osmotic pressure to the brush layer, and the counterions residing at the top of the brushes are driven into the brushes, which has denser chain segments and also slows the diffusion down. We believe that the latter scenario has more pronounced effect by the following consideration. Although the absolute values of diffusion coefficient of the probes differ by 2 orders of magnitude, their changes with the increase of salt concentration show almost an identical power index (~ 0.2),

while the thickness change with the salt level of these two systems exhibits a very big difference. If the nonuniform collapse imposes a bigger effect, the change of the D value with salt concentration should differ. The entering of the counterions relies on the salt concentration merely for both systems and should share a common feature. To fully discriminate between these two scenarios, a more systematic investigation is proceeding by further experiments with a different grafting density and controlled polydispersity.

CONCLUSION

By adopting ionic fluorescent molecules, sulforhodamine B and rhodamine 6G, as the probe for the counterions of the cationic PMETAC brushes and anionic PSS brushes, respectively, the diffusion of the counterions at the top of the brushes is successfully studied using single molecule fluorescence methods. The diffusivity of the ionic fluorophores serves as a sensitive probe for the distribution of the counterion of the polyelectrolyte brushes and also the structural change of the top part of the brushes. The sensitivity demonstrates the changes of the brushes with the change before the change of the whole brushes is detected by thickness measurements—the diffusion rate decreases at salt concentrations 3 orders of magnitude lower than that for the change of the thickness. The change of the diffusivity is attributed mainly to the process that the counterions are driven into the brushes by the osmotic pressure of the elevated salt concentration in the solution and less to the nonuniform collapse of the brushes. In both cases, the density of the chain segments around the probe becomes higher, which slows down the diffusion of the probes.

ASSOCIATED CONTENT

ⓢ Supporting Information. Video showing the diffusion of sulforhodamine B in PMETAC brushes (avi) and results of experiments using the sacrificial initiators. This material is available free of charge via the Internet at http://pubs.acs.org.

AUTHOR INFORMATION

Corresponding Author
*E-mail: jzhao@iccas.ac.cn.

ACKNOWLEDGMENT

REFERENCES

(1) Ballauff, M.; Borisov, O. *Curr. Opin. Colloid Interface Sci.* **2006**, *11*, 316.

(2) Rühe, J.; Ballauff, M.; Biesalski, M.; Dziezok, P.; Gröhn, F.; Johannsmann, D.; Houbenov, N.; Hugenberg, N.; Konradi, R.; Minko, S.; Motornov, M.; Netz, R. R.; Schmidt, M.; Seidel, C.; Stamm, M.; Stephan, T.; Usov, D.; Zhang, H. Polyelectrolyte brushes. *Adv. Polym. Sci.* **2004**, *165*, 189–198.

(3) Uhlmann, P.; Merlitz, H.; Sommer, J.-U.; Stamm, M. *Macromol. Rapid Commun.* **2009**, *30*, 732.

(4) Wittemann, A.; Ballauff, M. *Phys. Chem. Chem. Phys.* **2006**, *8*, 5269.

15172

dx.doi.org/10.1021/jp204612u |*J. Phys. Chem. B* 2011, 115, 15167–15173

(5) Jain, P.; Baker, G. L.; Bruening, M. L. *Annu. Rev. Anal. Chem.* **2009**, *2*, 387.

(6) Jusufi, A.; Likos, C. N.; Ballauff, M. *Colloid Polym. Sci.* **2004**, *282*, 910.

(7) Pincus, P. *Macromolecules* **1991**, *24*, 2912.

(8) Borisov, O. V.; Zhulina, E. B.; Birshtein, T. M. *Macromolecules* **1994**, *27*, 4795.

(9) Balastre, M.; Li, F.; Schorr, P.; Yang, J. C.; Mays, J. W.; Tirrell, M. V. *Macromolecules* **2002**, *35*, 9480.

(10) Leermakers, F. A. M.; Ballauff, M.; Borisov, O. V. *Langmuir* **2008**, *24*, 10026.

(11) Csajka, F. S.; Seidel, C. *Macromolecules* **2000**, *33*, 2728.

(12) Prabhu, V. M.; Vogt, B. D.; Wu, W. L.; Douglas, J. F.; Lin, E. K.; Satija, S. K.; Goldfarb, D. L.; Ito, H. *Langmuir* **2005**, *15*, 6647.

(13) Reznik, C.; Darugar, Q.; Wheat, A.; Fulghum, T.; Advincula, R. C.; Landes, C. *J. Phys. Chem. B* **2008**, *112*, 10890.

(14) Tran, Y.; Auroy, P. *J. Am. Chem. Soc.* **2001**, *123*, 3644.

(15) Moya, S. E.; Azzaroni, O.; Kelby, T.; Donath, E.; Huck, W. T. S. *J. Phys. Chem. B* **2007**, *111*, 7034.

(16) Wang, S. Q.; Zhao, J. *J. Chem. Phys.* **2007**, *126*, 091104.

(17) Magde, D.; Elson, E.; Webb, W. W. *Phys. Rev. Lett.* **1972**, *29*, 705.

(18) Rigler, R.; Widengren, J. *Bioscience* **1990**, *3*, 180.

(19) Sukhishvili, S. A.; Chen, Y.; Muller, J. D.; Gratton, E.; Schweizer, K. S.; Granick, S. *Nature* **2000**, *406*, 146.

(20) Zhao, J.; Granick, S. *Macromolecules* **2003**, *36*, 5443–5446.

(21) Bartko, A. P.; Xu, K.; Dickson, R. M. *Phys. Rev. Lett.* **2002**, *89*, 026101.

(22) Matyjaszewski, K.; Miller, P. J.; Shukla, N.; Immaraporn, B.; Gelman, A.; Luokala, B. B.; Siclovan, T. M.; Kickelbick, G.; Vallant, T.; Hoffmann, H.; Pakula, T. *Macromolecules* **1999**, *32*, 8716.

(23) Tran, Y.; Auroy, P.; Lee, L.-T. *Macromolecules* **1999**, *32*, 8952.

(24) Azzaroni, O.; Moya, S.; Farhan, T.; Brown, A. A.; Huck, W. T. S. *Macromolecules* **2005**, *38*, 10192.

(25) Farhan, T.; Azzaroni, O.; Huck, W. T. S. *Soft Matter* **2005**, *1*, 66.

(26) Yang, Q. B.; Zhao, J. *Langmuir* **2011**, *27*, 11757–11760.

(27) Patete, J.; Petrofsky, J. M.; Stepan, J.; Waheed, A.; Serafin, J. M. *J. Phys. Chem. B* **2009**, *113*, 583.

(28) Zhang, Y. J.; Cremer, P. S. *Curr. Opin. Chem. Biol.* **2006**, *10*, 658.

(29) Thomas, A. S.; Elcock, A. H. *J. Am. Chem. Soc.* **2007**, *129*, 14887.

(30) Geoghegan, M.; Ruiz-Peres, L.; Dang, C. C.; Parnell, A. J.; Martin, S. J.; Howse, J. R.; Jones, R. A. L.; Golestanian, R.; Topham, P. D.; Crook, C. J.; Ryan, A. J.; Sivia, D. S.; Webster, J. R. P.; Menelle, A. *Soft Matter* **2006**, *2*, 1076.

(31) Prabhu, V. M.; Rao, A.; Kang, S.; Lin, E. K.; Satija, S. K. *J. Phys. Chem. B* **2008**, *112*, 15628.